Available online at www.sciencedirect.com
ScienceDirect
Biochimica et Biophysica Acta 1768 (2007) 1567–1573
Biochimica et Biophysica Acta
BBA
www.elsevier.com/locate/bbamem

Oligomeric behavior of the RND transporters CusA and AcrB in micellar solution of detergent

David Stroebel [a,*], Véronique Sendra [a], Dominique Cannella [a,1], Kerstin Helbig [b], Dietrich H. Nies [b], Jacques Covès [a,*]

[a] *Laboratoire des Protéines Membranaires, Institut de Biologie Structurale, Jean-Pierre Ebel, UMR 5075 CNRS-CEA-UJF, 41, rue Jules Horowitz, 38027 Grenoble Cedex, France*
[b] *Institut für Mikrobiologie; Kurt-Mothes-Str. 3, D-06099 Halle, Germany*

Received 12 December 2006; received in revised form 12 February 2007; accepted 8 March 2007
Available online 24 March 2007

Abstract

We have used analytical ultracentrifugation to explore the oligomeric states of AcrB and CusA in micellar solution of detergent. These two proteins belong to the *r*esistance, *n*odulation and cell *d*ivision (RND) family of efflux proteins that are involved in multiple drug and heavy metal resistance. Only the structure of AcrB has been determined so far. Although functional RND proteins should assemble as trimers as AcrB does, both AcrB and CusA form a mixture of quaternary structures (from monomer to heavy oligomer) in detergent solution. The distribution of the oligomeric states was studied as a function of different parameters: nature and concentration of the detergent, ionic strength, pH, protein concentration. This pseudo-heterogeneity does not hamper the crystallization of AcrB as a homotrimer.

Keywords: RND transporter; Analytical ultracentrifugation; Detergent; Crystallization; Membrane protein; Oligomer

1. Introduction

As a Gram-negative bacterium, *Escherichia coli* contains seven multicomponent transporters of the *r*esistance, *n*odulation and cell *d*ivision (RND) family responsible for intrinsic drug tolerance [1,2]. Six efflux pumps confer resistance to a broad variety of compounds including antibiotics [3] and belong to the hydrophobic and amphiphilic efflux RND (HAE-RND) protein family. Together with a periplasmic membrane fusion protein (MFP) and an outer membrane factor (OMF), the resulting tripartite protein complex spans the complete cell wall of this bacterium and exports substrates probably from the periplasmic space to the outside. This process is driven by proton import, which is catalyzed by the inner membrane RND protein. An archetype of these efflux pumps is the homotrimeric RND protein AcrB that is associated with the MFP AcrA and the OMF TolC [4–6]. *E. coli* contains only one member of yet another RND protein family (heavy-metal efflux RND, HME-RND), CusA, which confers resistance to copper and silver [2,7]. CusA is encoded by the *cusCFBA* operon on the bacterial chromosome. In the respective transenvelope protein complex, CusB and CusC are the MFP and the OMF proteins, respectively. CusF is located in the periplasm and may serve as a kind of copper chaperone to deliver copper to CusA [8].

While HME-RND proteins were the first RND proteins described, a greater attention has been paid to HAE-RND proteins because of their high medical importance. For instance, the pathogenic bacterium *Pseudomonas aeruginosa* contains 13 RND transport systems and 12 of them are probably HAE-RND proteins [1]. This corresponds with an important role of RND

Abbreviations: AUC, analytical ultracentrifugation; DDM, *n*-dodecyl-*β*-D-maltopyranoside; FC14, *n*-tetradecylphosphocholine; FTIR, Fourier transform infrared spectroscopy; RND, resistance nodulation and cell division

* Corresponding authors. D. Stroebel is to be contacted at tel.: +33 1 44 32 38 88; fax: +33 1 44 32 38 94. J. Covès, tel.: +33 4 38 78 24 03; fax: +33 4 38 78 54 94.
E-mail addresses: david.stroebel@ens.fr (D. Stroebel), jacques.coves@ibs.fr (J. Covès).
[1] Present address: Laboratoire Adaptation et Pathogénie des Microorganismes Institut Jean Roget, Domaine de La Merci, 38700 Grenoble, France.

0005-2736/$ - see front matter © 2007 Elsevier B.V. All rights reserved.
doi:10.1016/j.bbamem.2007.03.008

proteins in antibiotic resistance of pathogenic bacteria in hospital environments and the related development of nosocomial diseases [9].

Although the atomic organization of HAE-RND proteins is now known with the X-ray structures of AcrB [10,11], such data are not yet available for HME-RND proteins. AcrB and CusA should have a similar topology and quaternary structure. However, our efforts to get structural data with CusA remained unproductive so far. We have thus used a series of techniques to compare back-to-back the behavior of these two proteins during purification by a protocol that yields AcrB crystals. Surprisingly, not only CusA (which did not crystallize so far) but also AcrB (which readily forms crystals) exist after purification as a mixture of oligomeric forms in detergent solution as shown by our analytical ultracentrifugation (AUC) data. This pseudo-heterogeneity does not hamper crystallization of AcrB as a homotrimer. We propose a mechanism that links the behavior of these oligomeric states and crystallization.

2. Materials and methods

2.1. Proteins, general techniques and crystallization

The AcrB overexpression vector is a kind gift of KM Pos. AcrB was purified as described in [12] except that *n*-dodecyl-β-D-maltopyranoside (DDM, Anatrace, CMC=0.17 mM or 0.0087%) was used instead of cyclohexyl-*n*-hexyl-*β*-D-maltoside. The construction of the CusA expression vector and the purification of CusA were as described in [13] for CzcA except that extra-phospholipids were not added during the solubilization or the purification steps. Alternatively, 0.4% *n*-dodecylphosphocholine (FC14, Anatrace, CMC=0.12 mM or 0.0046%) was used in place of DDM. Imidazole (AcrB) or desthiobiotine (CusA) were removed by cycles of concentration and dilution on Amicon cells equipped with YM-50 membranes. The final buffer contained either 0.02% DDM or 0.01% FC14.

Protein concentration was determined using bovine serum albumin as a standard and the Micro BCA protein assay (Pierce). Purity was estimated by 0.1% SDS–12% polyacrylamide gel electrophoresis. Oligomeric state was estimated by elution of a Superdex-200 filtration column calibrated with proteins of known hydrodynamic radius in detergent solution [14] or by sedimentation on sucrose density gradients formed by freeze–thawing treatment of 0.5 M sucrose in the suitable buffer [15]. One ml of protein solution was carefully loaded at the top of 10 ml sucrose gradients. The tubes were spun in a SW41 rotor (Beckman) during 16 h at 40,000 rpm. One ml fractions were collected from the top of the tubes before being analyzed by SDS-PAGE for protein content.

The amount of lipids in the protein preparations was checked by FTIR as described in [16] using an Avatar 330 (Thermo).

AcrB crystals were grown by sitting-drop vapor diffusion at 20 °C. A protein solution (15–20 mg/ml) was mixed at 1:1 ratio with the reservoir solution containing 16% PEG 2000, 10 mM sodium phosphate buffer pH 6.2 and 40 mM sodium citrate pH 5.6.

2.2. Analytical ultracentrifugation experiments

Sedimentation velocity experiments were performed in a Beckman XL-I analytical ultracentrifuge using a 4-hole or an 8-hole rotor (Beckman instruments), at 4 °C or 6 °C. Samples were handled immediately after purification and concentration on ultrafiltration membranes. In this case, a simple dilution in a chosen buffer allowed to study several parameters such as the protein and the detergent concentration. The pH value varied from 5.6 to 8 and the ionic strength from 0 to 500 mM NaCl.

Sedimentation velocity experiments were carried out at 42,000 rpm using 100 µl or 400 µl proteins samples, loaded in the two-channel 0.3 or 1.2 cm path length centerpieces, respectively. The buffer in the reference channel was identical with that of the sample but the detergent was omitted. Interference and absorbance (280 nm, with radial step size of 0.003 cm) scans were recorded overnight. Sedimentation velocity profiles were analyzed using the size distribution analysis from the program Sedfit (version 9.4b developed by P. Schuck and available at www.analyticalultracentrifugation.com). It provides a continuous distribution of apparent sedimentation coefficients, $c(s)$. The $c(s)$ analysis allows then to deconvolute the contribution of different species in a mixture [17,18]. About twenty regularly spaced experimental profiles were globally modeled. The $c(s)$ analysis was performed considering 200 particles on a grid of 300 radial points calculated with a frictional ratio f/f_0 of 1.25 and for sedimentation coefficient in the range of 1 to 50 S.

The density (ρ) and viscosity (η) of each solution were estimated with the program Sedentrp (available at http://www.jphilo.mailway.com/download.htm). The molar mass, molar extinction coefficient and partial specific volume of CusA and AcrB were deduced from their total amino-acid composition by the same program: CusA: 115,597 g/mol, 160,000 M^{-1} cm^{-1} and $\bar{V}$ 0.7456 ml/g (pI 5.92); AcrB: 114,654 g/mol, 90,100 M^{-1} cm^{-1} and $\bar{V}$ 0.7394 ml/g (pI 6.22). The partial specific volumes of detergents $\bar{V}_D$ used were: 0.824 ml/g for DDM and 0.94 ml/g for FC14 (considered here identical to FC12) [14]. The partial specific volume for the protein–detergent complex $\bar{V}_{PDC}$ was first considered to be 0.79 ml/g in DDM and 0.87 ml/g in FC14.

2.3. Analytical ultracentrifugation theory

The Svedberg equation relates the experimental s coefficient value to the buoyant molar mass of the protein detergent complex, Mb_{PDC}, and its Stoke radius Rs (N_A is Avogadro's number):

$$Mb_{PDC} = s\, N_A 6\pi\eta Rs \tag{1}$$

The value of the buoyant molar mass depends on the solvent density (δ) but can also be expressed as a function of the molecular mass of the protein (M_P), the quantity in g/g of bound detergent (γ_D), lipids (γ_L) and solvent (γ_W) per protein, and of $\bar{V}_P$, $\bar{V}_D$, $\bar{V}_L$ and $\bar{V}_w$:

$$Mb_{PDC} = M_P[(1-\delta\bar{V}_P) + \gamma_D(1-\delta\bar{V}_D) + \gamma_L(1-\delta\bar{V}_L) + \gamma_w(1-\delta\bar{V}_w)] \tag{2}$$

Contribution of solvent has been neglected here.

Particles that contributes only to interference signal could be quantified by measuring the number of recorded fringes, that is linked to concentration by the following equation:

$$J = dn/dc \cdot c \cdot / \cdot \lambda / K \tag{3}$$

where, c the concentration of particle, l the path length, the wavelength λ=675 nm, the constant K=1.013, dn/dc the interference contribution of the particle : 0.186 ml/g for a protein (J/c of 2.76) and 0.133 ml/g for both detergent DDM and FC14.

The amount of surfactant associated with the protein $\gamma_T=(\gamma_D+\gamma_L)$ was estimated by quantitative comparison of $c(s)$ analysis between absorbance and interference data. If we neglect the contribution of lipids (no or few associated lipids):

$$\gamma_D = ((J \cdot \varepsilon_{M280\ nm}/DO_{280\ nm}) - J/c_{protein})/J/c_{detergent}. \tag{4}$$

3. Results

3.1. Purification, homogeneity, stability and crystallization

CusA was purified by affinity chromatography on a streptactin-column after solubilization with DDM (Fig. 1A). Detergent FC14 could also be used for solubilization and purification. Both detergents kept CusA in solution. The molecular mass of CusA was determined as about 110,000 Da

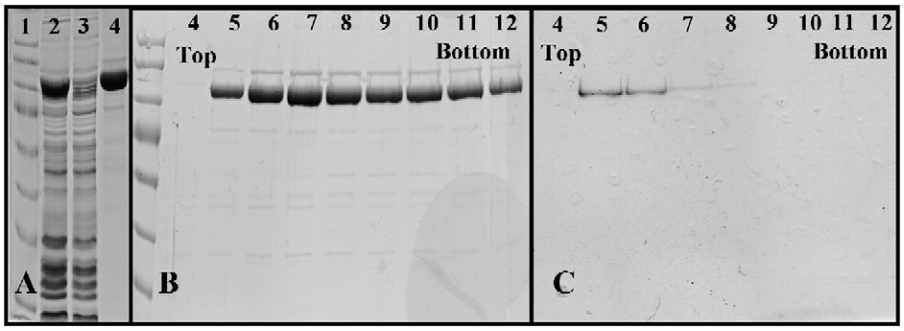

Fig. 1. SDS-PAGE analysis of different CusA preparations. Panel A, purification of CusA: 1, molecular mass markers; 2, membrane preparation; 3, flow through of the strep-tag affinity column; 4, desthiobiotin elution of CusA from the strep-tag affinity column. Panel B, DDM–CusA on sucrose density gradient containing 0.05% of DDM. Panel C, FC14–CusA on sucrose density gradient containing 0.025% of FC14. Only fractions 4 to 12 were used for the SDS-PAGE analysis.

by SDS-PAGE analysis. This value agrees well to a mass of 114,707 Da deduced from the predicted amino acid sequence.

Homogeneity of the protein preparations was investigated by sucrose density gradient centrifugations followed by SDS-PAGE analysis of the fractions (Fig. 1B). After 16 h of centrifugation at 40,000 rpm, CusA solubilized with DDM (DDM–CusA in the following) was present in fractions 5 to 12. This strongly suggests that CusA existed in solution as a mixture of different oligomeric states and not as a mere trimer as expected for a RND protein according to the AcrB structure. The CusA preparation obtained in the presence of FC14 (FC14–CusA in the following) was much more homogeneous as CusA was obtained in fractions 5 and 6 essentially (Fig. 1C). Detection of CusA in these two fractions from the top of the gradient indicated the presence of simpler and smaller quaternary CusA structures in FC14 preparations compared to DDM preparations. As estimated from the position of FC14–CusA in the sucrose gradient after centrifugation, FC14–CusA could be a simple monomer while the DDM preparations contained CusA multimers. Interestingly, regardless of the storage condition, DDM–CusA was stable for weeks whereas FC14 preparations were quickly denatured, probably by proteolysis (not shown).

Purified DDM–AcrB preparations were also stable for weeks (not shown). AcrB crystallized under conditions similar to those already described [5,19]. The resulting crystals diffracted on the ESRF beamline ID29 and gave identical space group and cell parameters as previously obtained [20]. Sometimes, two types of crystals were present in the same drop (see picture in Fig. 5). This was also in agreement with even three types of crystals grown in the same drop (K.M. Pos, personal communication). Thus, CusA and AcrB could be purified easily after solubilization with DDM and both proteins were stable for weeks. However, AcrB crystallized easily but CusA did not.

3.2. Behaviors of AcrB and CusA in detergent solution

Data from dynamic light scattering, electron microscopy and size exclusion chromatography confirmed the heterogeneity of the solubilized CusA preparations. Thus, CusA and AcrB micellar solutions were compared by AUC. Detergent-solubilized membrane proteins in micellar solution may form complicated complexes composed of protein, detergent and lipids. Nevertheless, molecular masses could be calculated from the sedimentation coefficients if a globular structure of the particle was assumed and the amount of surfactant of the protein–detergent complex was also taken into consideration. To obtain this information the concentration of detergent free micelles was deduced from interference data (Fig. 2) and subtraction of the protein concentration to this interference data gave the amount of detergent linked to each complex (Eqs. (3) and (4)) [21].

AUC analysis of FC14–CusA revealed the presence of one species ($s_{20,w}$ of 5.5 S) associated with 1.8±0.6 g of detergent per g of protein (Fig. 2A). Solution of Eqs. (1) and (2) yielded a molecular mass that was only compatible with the monomeric form of CusA. This result agreed with that from sucrose density gradient centrifugation.

DDM preparations of CusA and AcrB gave both three distinct major species with $s_{20,w}$ values of 8 S, 11 S and 16 S respectively, along with heavier species (Fig. 2B and C). These $s_{20,w}$ values of these heavier species could not be determined precisely. All $s_{20,w}$ values were obtained in twenty AUC experiments and gave reproducible results, strongly indicating that the presence of these discrete species were no artefacts. The mean value for the amount of complex-associated detergent was similar for the three major species, 1.5±0.6 g per g of protein for DDM–CusA and 1.2±0.4 g per g of protein for DDM–AcrB.

The presence and the amount of lipids in the protein preparations were determined by FTIR analysis (Fig. 3). The surface ratios between the peak of carboxylic amide at 1755 cm^{-1} (corresponding to protein) and that of carboxylic ester at 1740 cm^{-1} (lipids) [16] gave an estimate of 5 to 10 lipids per protein for DDM–CusA. In case of AcrB, no peak could be detected at 1740 cm^{-1} (Fig. 3), suggesting a maximum of 2 lipids per protein.

Using the values for the amount of complex-associated detergent and that of lipids in the protein preparations, theoretical $s_{20,w}$ values for monomeric, dimeric and trimeric DDM–CusA in spherical protein–detergent–lipid particles were calculated as 9.2±1 S, 14.6±1.5 S and 19.7±2 S, respectively. The same calculation for AcrB gave rather similar results of 9±1 S, 14.3±1.5 S and 18.8±2 S respectively.

When the Hydropro software [22] was used to calculate the Stokes radius of AcrB (pdb entry 1T9T) in the absence of

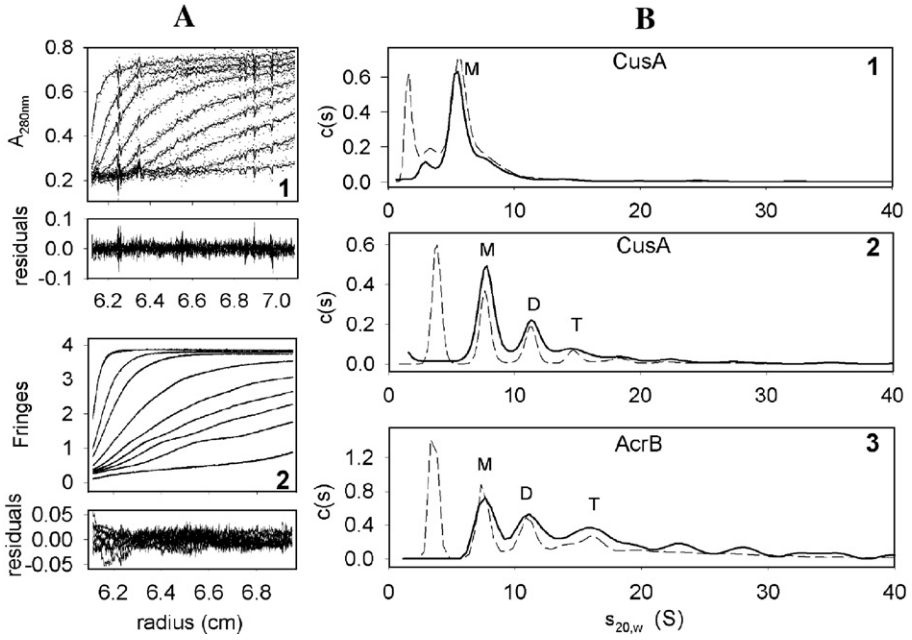

Fig. 2. Sedimentation velocity of different CusA or AcrB preparations. Data were recorded in absorbance (Panel A, 1) and in interference (Panel A, 2). The corresponding residuals represent the superimposition of the differences between the experimental and fitted curves. Panel B, $c(s)$ analysis for 1, 5.6 μM CusA in 6.7 mM FC14 at 4 °C; 2, 5.6 μM CusA in 2.1 mM DDM at 6 °C and 3, 4.9 μM AcrB in 0.7 mM DDM at 6 °C. Interference data are in dotted line while A_{280} data are in solid line. The peaks observed in interference only correspond to the free detergent micelles. M is for monomer, D for dimer and T for trimer.

detergent, the result was 4.5 nm for the monomer and 6 nm for the trimer. On the other hand, Stokes radii of 4.03 nm for the monomer and 5.82 nm for the trimer were used to compute the theoretical $s_{20,w}$ values. Therefore, the theoretical $s_{20,w}$ values should be higher than those experimentally determined and, with some confidence, the 8 S species could be assigned to the monomeric form of CusA or AcrB, respectively. Furthermore, the 11 S species in both protein preparations should represent dimers and the 16 S species trimers. The additional high molecular mass signals with $s_{20,w}$ values between 19 S and 47 S, which could not be separated into single signals and described precisely, may represent a mixture of various oligomers larger than trimers.

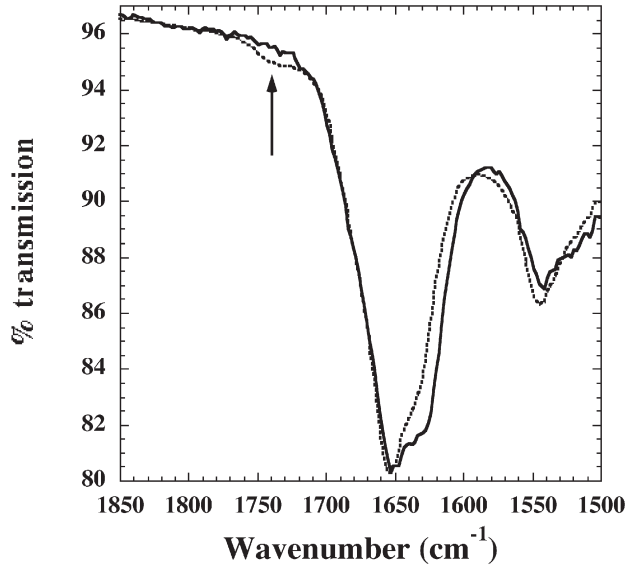

Fig. 3. FTIR spectra of dried DDM CusA and AcrB preparations. Spectra were recorded as described in [16]. Solid line is for AcrB and dotted line for CusA. The arrow indicates the resonance peak of the ester carbonyl characteristic of the presence of lipids, visible in DDM–CusA.

The overall sedimentation profiles of DDM–AcrB and DDM–CusA were reproducible and, compared to each other, very similar. In all protein preparations, monomers, dimers, trimers and heavier oligomers were observed (Fig. 4). However, the relative proportion of each population varied with the experimental conditions, e.g. the protein, salt or detergent concentration (Fig. 4). The heavy oligomers were the most abundant AcrB population except at high salt concentrations while the monomeric form of CusA was dominant except under high protein concentrations. At high salt concentrations, both AcrB and CusA were predominantly present in their monomeric forms (Fig. 4A, condition 3; Fig. 4B, condition 1). The species distribution for DDM–AcrB was poorly affected by the detergent concentration (Fig. 4A, conditions 4 and 5). No difference in $c(s)$ distribution profiles was observed within pH ranges from 6 to 8 (not shown) or after incubation for 72 h at 4 °C for both AcrB and CusA.

An increase in the protein concentration raised the portion of the heavy 19–47 S oligomers in case of AcrB and of CusA (Fig. 4A and B, conditions 2) but for AcrB more than for CusA. It should be noted that the parameters of condition 4 for DDM–AcrB were closest to those leading to crystallization of this protein.

4. Discussion

The only structure of an RND transporter solved so far is that of AcrB. This protein can be purified in large amounts. It

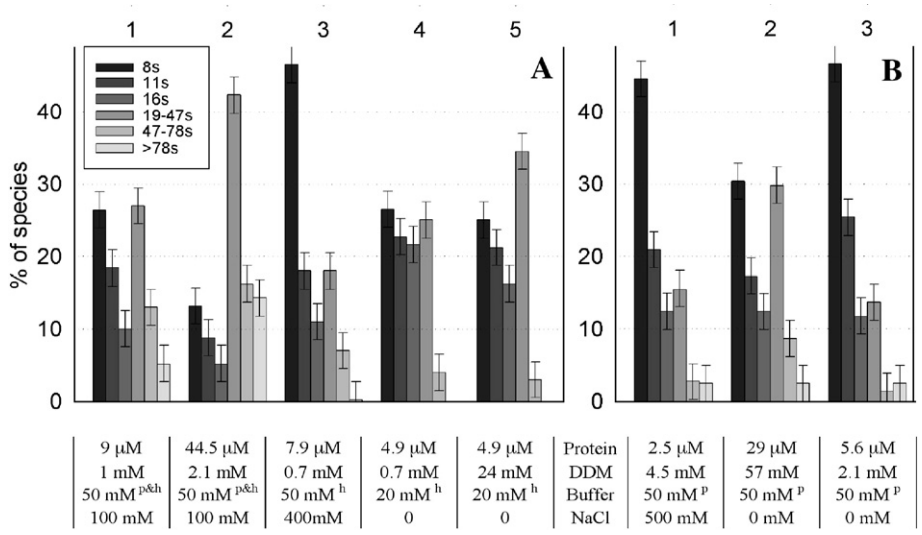

Fig. 4. Distribution of the oligomeric states for AcrB (Panel *A*) and CusA (Panel B) deduced from AUC experiments. Populations have been sorted as follows: 8 S, 11 S and 16 S correspond to discrete species and are respectively for the monomers, the dimers and the trimers. Heavier species are defined as a population comprised between two given S values. Percentages are calculated by ratio of the observed peak area on the total area of the curve (Fig. 2). Protein concentration was estimated from A_{280}. The free DDM concentration was calculated by contribution of interference on micelles peak (Eq. (3)). For buffers, ^{p} indicates the use of phosphate buffer pH 7 and ^{h} that of HEPES buffer pH 8. Error bars represent the uncertainty in the choice of the integration limits for each species in the $c(s)$ analysis.

is stable and crystallizes easily. The first structures were obtained from crystals grown in a trigonal *R*32 space group with trimers of AcrB being centered on the crystallographic three-fold axis [5,19,20]. Consequently, the three monomers had a strictly similar conformation and the question of how AcrB can actively export a wide variety of toxic compounds remained unanswered. Two recent papers describe AcrB structures solved from crystals belonging to the monoclinic *C*2 or the triclinic *P*1 space group, respectively [10,11]. In these crystals each monomer can take three independent conformations. Analyses of these new structures led to the proposal of a three-step rotation mechanism of drug efflux in a kind of peristaltic mode [10,11]. Anyway, the new structures are basically consistent with the previous ones and confirm that the functional unit of AcrB is the trimer. As suggested from sequence similarities and function analogy, it appears necessary for RND proteins to assemble into trimer as the active form for substrate transport.

To study the oligomeric state of detergent-solubilized RND proteins in solution, the HAE-RND model protein AcrB was compared to CusA, an RND protein of the HME-RND family. Both RND proteins were present as highly polydisperse distributions in micellar solutions of DDM. Detailed analysis of data obtained by analytical ultracentrifugation demonstrated the co-existence of a large range of oligomeric forms from monomers to dimers, trimers and not very well defined heavy oligomers larger than trimers. Since CusA and AcrB belong to different families of the RND superfamily and share only a limited degree of similarity (22% identity on the amino acid level), this peculiar behavior could be a general feature of all members of the RND transporter superfamily.

MexB from *P. aeruginosa* is another HAE-RND protein and a close AcrB homologue. Purified MexB was proposed to exist as a homotrimer in DDM solution with 398±12 DDM molecules bound to each MexB molecule [23]. Thus, DDM would contribute a molecular mass of 203.2±6.1 kDa per MexB monomer (112.8 kDa) to the total molecular mass of the DDM–protein complex, leading to a molecular mass of about 948 kDa of the trimeric $(DDM–MexB)_3$ complex. Such a complex would have a Stokes radius of 8.34 nm and a $s_{20,w}$ value of 20.1 S but instead 6.02 nm and 13.8 S, respectively, were experimentally determined [23]. This could indicate the presence of low molecular mass species, e.g. monomers and dimers, in the MexB preparation as well.

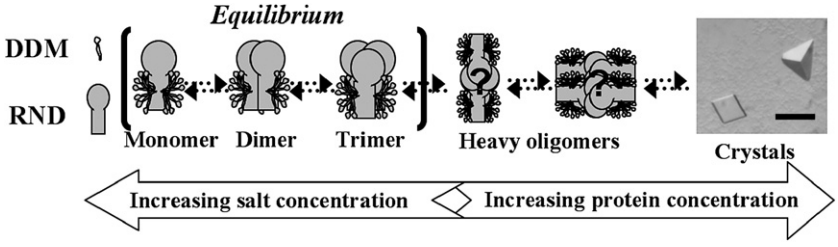

Fig. 5. Schematic representation of the oligomeric equilibrium leading to crystallization of RND transporters. AcrB crystals were obtained in the crystallization conditions indicated in Materials and methods. Solid bar in the picture on the right corresponds to 150 µm.

DDM–AcrB and DDM–CusA formed in solution discrete protein species. The sedimentation coefficients of the monomeric, dimeric and trimeric forms were identical under various experimental conditions, although the relative amounts of these species varied with some conditions, e.g. salt, protein and DDM concentration. However, under a given condition the portion of each species was stable with time, up to 72 h, and did not depend on the protein concentration when only the monomers, dimers and trimers were considered (Fig. 4). This strongly suggests that the monomers, dimers and trimers were in a slow association and dissociation equilibrium [24] (Fig. 5).

Although the detergent concentration slightly increased the amount of AcrB and CusA in the heavy oligomeric form with $s_{20,w}$ values between 19 S and 47 S, this parameter did not effect the distribution of either protein between the monomeric, dimeric and trimeric forms (Fig. 4). This was a surprise and contrary to observation from other membrane proteins [25,26]. Since the equilibrium between these three forms was primarily sensitive to the protein concentration and ionic strength, the soluble domains of RND proteins should be primarily responsible for associations into larger structures. In agreement with this suggestion, the three AcrB polypeptides in the homotrimer interact mainly by large contacts between their periplasmic domains, with only few contacts between the membrane domains.

The heavy oligomeric forms (19 S to 47 S) of AcrB and CusA were always present. In case of AcrB, this form was predominant in conditions that led to crystallization. This suggests that this oligomeric form did not correspond to denatured and aggregated protein but could rather be an intermediate on the way to crystallization (Fig. 5). Since the portion of this large species increased with rising protein concentration and the protein concentration itself increases in the crystallization process when the hanging drop loses water as vapor, the heavy oligomeric forms could play a crucial role in nucleation and growth of the crystals (Fig. 5). Indeed, some membrane protein preparations could become more polydisperse when the protein concentration increases [27] and polydispersity of soluble proteins exists even in supersaturating conditions [28,29], i.e. above the boundary of the solubility curve corresponding to the liquid–liquid phase separation in protein phase diagrams.

Although AcrB and CusA belong to the same protein superfamily, share a similar function and a rather similar behavior in detergent solution, we have not been able to obtain CusA crystals. This can be explained by the low percentage of identity between the two proteins, leading to differences in the solvent exposed surfaces. Some other differences between CusA and AcrB preparations can also be noted. The CusA protein cannot be concentrated without concentrating the detergent at the same time. This may be related to the fact that purified CusA contained some lipids as seen by FTIR analysis. AcrB did not and can be concentrated easily. Moreover, at low protein concentrations, the portion of monomeric DDM–CusA is higher than that of monomeric DDM–AcrB (Fig. 4), which adds to the reluctance of CusA against crystallization. Greater independence of monomeric DDM–CusA may be an intrinsic property of this protein. Aggregation of RND proteins into trimers may be initiated by intertwining loops of the protomers (corresponding to the loop at amino acid position 212–239 in AcrB). This loop is 6-amino acids shorter in CusA than in AcrB. This could make more difficult the association of CusA into dimers, trimers and heavier oligomers. Accordingly and because FC14 has a stronger dissociating effect than DDM, FC14–CusA preparation was predominantly in the monomeric form that was highly sensitive to proteolytic degradation.

In conclusion, pseudo-heterogeneity of the AcrB preparations was not a contra-indication for crystallization. On the contrary, behavior of DDM–AcrB in conditions that led to crystallization suggests that it is not only necessary to avoid monomerization (use of dissociating detergent or high salt concentration) but furthermore to reach a protein concentration that allows the formation of a mixture of oligomeric forms, including high molecular mass oligomers that could trigger the nucleation. In other words, the quest for the monodispersity is not the good solution to crystallize AcrB or other RND transporters.

Acknowledgments

We are grateful to Dr. C. Ebel for her help during AUC experiments and interpretation of the AUC data, to Dr. KM Pos for giving us the AcrB overproduction plasmid, to Dr. D. Gaude for access to the FTIR device and to Drs J. Baenziger and J. Sturgis for their help in interpretation of the FTIR data. DS and VS are fellows of the Programme National de Toxicologie Nucléaire Environnementale. This study was also supported by a DFG grant to DHN (Ni262/3) and a PROCOPE grant to JC and DHN for French-German cooperation.

References

[1] D.H. Nies, Efflux-mediated heavy metal resistance in prokaryotes, FEMS Microbiol. Rev. 27 (2003) 313–339.
[2] T.T. Tseng, K.S. Gratwick, J. Kollman, D. Park, D.H. Nies, A. Goffeau, M.H. Saier Jr., The RND permease superfamily: an ancient, ubiquitous and diverse family that includes human disease and development proteins, J. Mol. Microbiol. Biotechnol. 1 (1999) 107–125.
[3] L.J. Piddock, Multidrug-resistance efflux pumps—not just for resistance, Nat. Rev., Microbiol. 4 (2006) 629–636.
[4] H. Nikaido, Multidrug efflux pumps of gram-negative bacteria, J. Bacteriol. 178 (1996) 5853–5859.
[5] S. Murakami, R. Nakashima, E. Yamashita, A. Yamaguchi, Crystal structure of bacterial multidrug efflux transporter AcrB, Nature 419 (2002) 587–593.
[6] E.B. Tikhonova, H.I. Zgurskaya, AcrA, AcrB, and TolC of *Escherichia coli* form a stable intermembrane multidrug efflux complex, J. Biol. Chem. 279 (2004) 32116–32124.
[7] C. Rensing, G. Grass, *Escherichia coli* mechanisms of copper homeostasis in a changing environment, FEMS Microbiol. Rev. 27 (2003) 197–213.
[8] S. Franke, G. Grass, C. Rensing, D.H. Nies, Molecular analysis of the copper-transporting efflux system CusCFBA of *Escherichia coli*, J. Bacteriol. 185 (2003) 3804–3812.
[9] L.J. Piddock, Clinically relevant chromosomally encoded multidrug resistance efflux pumps in bacteria, Clin. Microbiol. Rev. 19 (2006) 382–402.
[10] M.A. Seeger, A. Schiefner, T. Eicher, F. Verrey, K. Diederichs, K.M. Pos,

Structural asymmetry of AcrB trimer suggests a peristaltic pump mechanism, Science 313 (2006) 1295–1298.
[11] S. Murakami, R. Nakashima, E. Yamashita, T. Matsumoto, A. Yamaguchi, Crystal structures of a multidrug transporter reveal a functionally rotating mechanism, Nature 443 (2006) 173–179.
[12] K.M. Pos, K. Diederichs, Purification, crystallization and preliminary diffraction studies of AcrB, an inner-membrane multi-drug efflux protein, Acta Crystallogr., D Biol. Crystallogr. 58 (2002) 1865–1867.
[13] M. Goldberg, T. Pribyl, S. Juhnke, D.H. Nies, Energetics and topology of CzcA, a cation/proton antiporter of the resistance-nodulation-cell division protein family, J. Biol. Chem. 274 (1999) 26065–26070.
[14] M. le Maire, P. Champeil, J.V. Moller, Interaction of membrane proteins and lipids with solubilizing detergents, Biochim. Biophys. Acta 1508 (2000) 86–111.
[15] P. Fourcroy, S. Cuiller, F.C. Largitte, C. Lambert, Polyribosome analysis on sucrose gradients produced by the freeze–thaw method, J. Biochem. Biophys. Methods 4 (1981) 243–246.
[16] C.J. daCosta, J.E. Baenziger, A rapid method for assessing lipid:protein and detergent:protein ratios in membrane–protein crystallization, Acta Crystallogr., D Biol. Crystallogr. 59 (2003) 77–83.
[17] P. Schuck, Size-distribution analysis of macromolecules by sedimentation velocity ultracentrifugation and lamm equation modeling, Biophys. J. 78 (2000) 1606–1619.
[18] P.H. Brown, P. Schuck, Macromolecular size-and-shape distributions by sedimentation velocity analytical ultracentrifugation, Biophys. J. 90 (2006) 4651–4661.
[19] E.W. Yu, G. McDermott, H.I. Zgurskaya, H. Nikaido, D.E. Koshland Jr., Structural basis of multiple drug-binding capacity of the AcrB multidrug efflux pump, Science 300 (2003) 976–980.
[20] K.M. Pos, A. Schiefner, M.A. Seeger, K. Diederichs, Crystallographic analysis of AcrB, FEBS Lett. 564 (2004) 333–339.
[21] E. Cohen, R. Goldshleger, A. Shainskaya, D.M. Tal, C. Ebel, M. le Maire, S.J. Karlish, Purification of Na+,K+-ATPase expressed in *Pichia pastoris* reveals an essential role of phospholipid–protein interactions, J. Biol. Chem. 280 (2005) 16610–16618.
[22] J. Garcia De La Torre, M.L. Huertas, B. Carrasco, Calculation of hydrodynamic properties of globular proteins from their atomic-level structure, Biophys. J. 78 (2000) 719–730.
[23] V. Mokhonov, E. Mokhonova, E. Yoshihara, R. Masui, M. Sakai, H. Akama, T. Nakae, Multidrug transporter MexB of *Pseudomonas aeruginosa*: overexpression, purification, and initial structural characterization, Protein Expr. Purif. 40 (2005) 91–100.
[24] P. Schuck, On the analysis of protein self-association by sedimentation velocity analytical ultracentrifugation, Anal. Biochem. 320 (2003) 104–124.
[25] D. Josse, C. Ebel, D. Stroebel, A. Fontaine, F. Borges, A. Echalier, D. Baud, F. Renault, M. Le Maire, E. Chabrieres, P. Masson, Oligomeric states of the detergent-solubilized human serum paraoxonase (PON1), J. Biol. Chem. 277 (2002) 33386–33397.
[26] L.E. Fisher, D.M. Engelman, J.N. Sturgis, Effect of detergents on the association of the glycophorin a transmembrane helix, Biophys. J. 85 (2003) 3097–3105.
[27] A. Zouni, J. Kern, J. Frank, T. Hellweg, J. Behlke, W. Saenger, K.D. Irrgang, Size determination of cyanobacterial and higher plant photosystem II by gel permeation chromatography, light scattering, and ultracentrifugation, Biochemistry 44 (2005) 4572–4581.
[28] C. Hamiaux, J. Perez, T. Prange, S. Veesler, M. Ries-Kautt, P. Vachette, The BPTI decamer observed in acidic pH crystal forms pre-exists as a stable species in solution, J. Mol. Biol. 297 (2000) 697–712.
[29] W. Kadima, A. McPherson, M.F. Dunn, F.A. Jurnak, Characterization of precrystallization aggregation of canavalin by dynamic light scattering, Biophys. J. 57 (1990) 125–132.